Conversion of a bio-oil model compound on $AlCl_3$-modified porous catalysts investigated by in situ multi-nuclear solid-state NMR spectroscopy

S. Lang, M. Heuchel, E. Klemm, M. Hunger

Institute of Chemical Technology, University of Stuttgart, 70569 Stuttgart, Germany

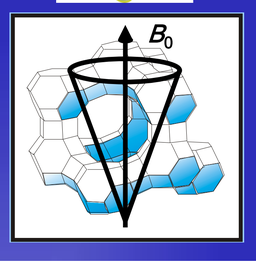

Introduction

The energy demand of our society is secured by a high proportion of the fluid catalytic cracking process of fossil-based vacuum gas oil. The future implementation of the FCC process probably contains a blend of vacuum gas oil and lignin-based bio-oil. Thereby, the greenhouse gas emission could decreased and the content of renewable energy resources increased. This are self-imposed targets of the European Union (EU) and part of the 20-20-20 goal to prevent a dangerous climate change [1]. In more detail, the EU plans the decrease of greenhouse gas emission by 20 % (from 1990 levels) and improve the energy efficiency and the content of renewable energy sources also by 20 % until the year 2020. The co-feeding of bio-oil compounds, however, requires optimizing the performance of the FCC catalysts due to the high content of oxygen and the sterically demanding molecules in the slightly hydrodeoxygenated bio-oil. Therefore, the co-FCC catalysts have to be coke selective with high hydrothermal stability and catalytic activity. Typical FCC catalysts are a mixture of ultra stable zeolite Y (USY) with high pore area and acid density and strength, a matrix and additives like ZSM-5. By modifications like chemically leaching and steaming of USY catalysts, the acid site density decreases. Inversely, new acid sites could created with $AlCl_3$-modification of porous Si-rich materials [2]. The post-synthetic formation of surface acid sites was investigated with solid-state NMR. The catalytic cracking performance of parent and $AlCl_3$-modified catalysts were carried out under batch conditions with pure 2-ethylphenol as bio-oil model compound and were investigated with in situ solid-state NMR spectroscopy.

Experimental

The synthesis of the parent SBA-15 was carried out as described by Zhao et al. [3]. Parent dealuminated zeolite Y (DeaY) and USY were delivered by Degussa AG and Grace GmbH & Co KG, respectively. The material USY was also treated for 1 h with 0.2 M HCl and after washing and drying treated with 0.5 NaOH-solution at room temperature. Subsequently, an ion-exchange at 353 K with 1 M NH_4NO_3-solution was done to transfer the zeolite in its protonated form. The ion-exchange was two times repeated. The chemically leached material is denoted as USY*. The $AlCl_3$-modification of the parent porous materials was performed under batch conditions in glass tubes with a diameter of 4 mm. Therefore, the anhydrous $AlCl_3$ (Acros Organics) was put at the bottom of the tubes, while hydrated parent materials were situated above. The weight ratios of porous material and $AlCl_3$ was 5:1. The $AlCl_3$ was sublimated via heating with a rate of 2 K/min up to 393 K and simultaneous evacuation ($p < 10^{-2}$ mbar) for 2 h. Afterwards, the tubes were sealed and heated at 423 K for 36 h. Samples after this step are denoted as "parent material/$AlCl_3$/423". For a second modification step, some of the before mentioned samples were hydrated for 4 h in a desiccator over saturated solution of $Ca(NO_3)_2$ and subsequently calcined at 723 K with simultaneously evacuation ($p < 10^{-2}$ mbar). This samples are denoted as "parent material/$AlCl_3$/723". Dehydrogenated parent and modified materials were loaded with 2-ethylphenol (99 %, Sigma Aldrich) in a glovebox purged with dry nitrogen. The loading was carried out with a syringe and according to ^{1}H MAS NMR the value of loading was 0.8 – 1.2 mmol g^{-1}. Afterwards, the loaded materials were sealed in glass tubes after a short evacuation. The reaction takes place in these sealed glass tubes at 753 K for 10 min. The organic residue were studied with ^{1}H and ^{13}C MAS NMR as well as ^{1}H spin echo NMR spectroscopy.

Results and Discussion

Characterization of $AlCl_3$-modified materials

^{27}Al MAS NMR spectroscopy

In Figures 1a and 2a of the Si-rich materials SBA-15 and DeaY are only very weak ^{27}Al MAS NMR signals due to the low aluminum content. Due to the modification with $AlCl_3$ onto the parent Si-rich materials and heating at 423 K, additional strong signals at δ_{27Al} = 0 ppm appear in Figures 1b and 2b. This signals are due to octahedrally coordinated aluminum on the surface of the porous materials. Typical signals of $AlCl_n$ with chemical shifts of δ_{27Al} = 90 - 110 ppm are not observable [4]. Due to the calcination at 723 K in vacuum, the octahedrally coordinated aluminum is redistributed evidenced by the strong decrease of the Al^{VI} signal at δ_{27Al} = 0 ppm, the appearance of a weak signal of Al^{V} at δ_{27Al} = 35 ppm, and a significant increase of the framework aluminum species Al^{IV} at δ_{27Al} = 53 and 58 ppm for SBA-15/$AlCl_3$/723 and DeaY/$AlCl_3$/723, respectively (Fig. 1c and 2c).

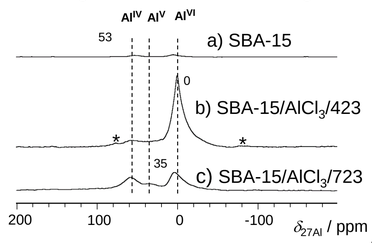

Fig 1: ^{27}Al MAS NMR spectra of hydrated SBA-15 before (a) and after $AlCl_3$ modification at 423 K (b) and 723 K (c). *Asterisks* denote spinning sidebands.

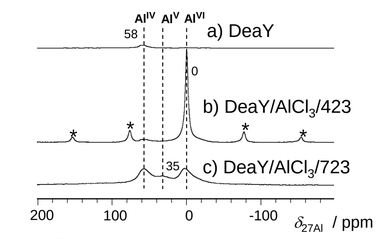

Fig 2: ^{27}Al MAS NMR spectra of hydrated DeaY before (a) and after $AlCl_3$ modification at 423 K (b) and 723 K (c). *Asterisks* denote spinning sidebands.

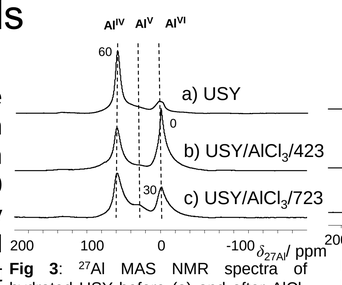

Fig 3: ^{27}Al MAS NMR spectra of hydrated USY before (a) and after $AlCl_3$ modification at 423 K (b) and 723 K (c).

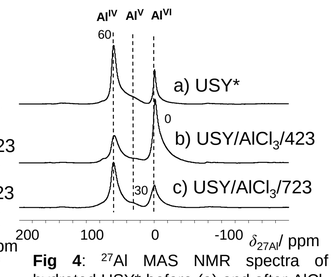

Fig 4: ^{27}Al MAS NMR spectra of hydrated USY* before (a) and after $AlCl_3$ modification at 423 K (b) and 723 K (c).

For Al-rich materials USY and USY*, the effect of $AlCl_3$-modification differs to Si-rich materials. The dominating signal in Figure 3a and 4a at δ_{27Al} = 60 ppm for framework Al^{IV} aluminum decrease due to the $AlCl_3$-modification and heating at 423 K (Fig. 3b and 4b). However, signal intensities of octahedrally coordinated Al^{VI} aluminum at δ_{27Al} = 0 ppm on USY and USY* increases. Due to the calcination at 723 K in vacuum, the octahedrally coordinated aluminum is again re-distributed. Similar to Si-rich materials, the signal at δ_{27Al} = 0 ppm for octahedrally coordinated aluminum decreases significant and simultaneous the intensities of framework aluminum at δ_{27Al} = 60 ppm increases for USY/$AlCl_3$/723 and USY*/$AlCl_3$/723 in Figures 3c and 4c.

Tab. 1: Bulk n_{Si}/n_{Al} ratios, Brønsted and Lewis acid site density of parent and modified porous materials under study.

Porous materials	Bulk ratio n_{Si}/n_{Al} by ICP-OES	n_{NH4+} a) / mmol g^{-1}	n_{NH3} a) / mmol g^{-1}
SBA-15	≅ 600	n.s.o.	n.s.o.
SBA-15/$AlCl_3$/423	11	0.045	0.110
SBA-15/$AlCl_3$/723	10	0.020	0.165
DeaY	116	0.015	0.005
DeaY/$AlCl_3$/423	21	0.005	0.080
DeaY/$AlCl_3$/723	20	0.035	0.100
USY	2.9	0.972	0.185
USY/$AlCl_3$/423	2.6	0.801	0.039
USY/$AlCl_3$/723	2.7	0.400	0.324
USY*	3.3	0.730	0.121
USY*/$AlCl_3$/423	3.5	1.364	0.017
USY*/$AlCl_3$/723	3.3	0.437	0.271

n.s.o. no signal observable
a) Experimental accuracy of ± 10%

^{1}H MAS NMR spectroscopy

The investigation of acid sites densities was carried out with ammonia as probe molecule and quantitative solid-state ^{1}H NMR spectroscopy. Therefore, ammonia was adsorbed on dehydrated materials under study and the integrals of characteristic ^{1}H MAS NMR shifts of ammonium ions formed at Brønsted acid sites (BAC) (δ_{1H} = 6 – 7 ppm) and ammonia molecules coordinated at Lewis acid sites (LAC) (δ_{1H} = -0.5 to 3.0 ppm) received of the difference spectra of unloaded and ammonia loaded ^{1}H MAS NMR spectra were compared with an external intensity standard sample (H,Na-Y with 1.776 mmol g^{-1} OH groups). In Figure 5 is an example of the spectra subtraction of ammonia loaded and unloaded DeaY. The determined acid site densities of the materials under study are given in Table 1. Especially LAC were formed by $AlCl_3$-modification on parent materials under study.

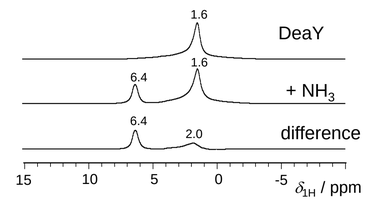

Fig 5: ^{1}H MAS NMR spectra of dehydrated DeaY (top) and ammonia loaded DeaY (middle) The bottom spectra (difference) were obtained via subtracting the top from the medium spectra.

Conversion of 2-ethylphenol on parent and $AlCl_3$-modified materials

^{1}H spin echo NMR spectroscopy

The investigation of the volatile reaction products after the conversion of 2-ethylphenol (EP) was studied with ^{1}H spin echo NMR spectroscopy. In Figure 6 and 7 a scheme of the utilized ^{1}H spin echo NMR technique and the plus sequence of this experiments are shown, respectively. After the reaction of EP on materials under study, the main volatile products in the sealed glass tubes are methane (δ_{1H} = 0.2 ppm), ethane (δ_{1H} = 0.9 ppm) and –CH_2– groups (δ_{1H} = 1.2 ppm) (Fig. 8).

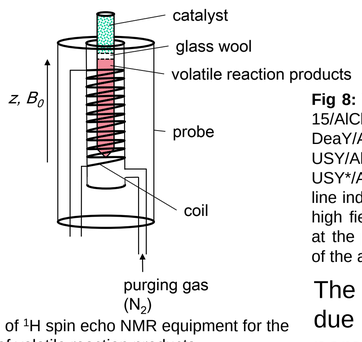

Fig 6: Scheme of ^{1}H spin echo NMR equipment for the measurement of volatile reaction products.

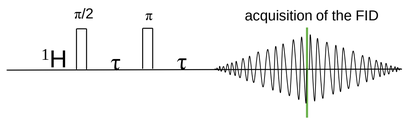

Fig. 7: Puls sequence of ^{1}H spin echo NMR experiments.

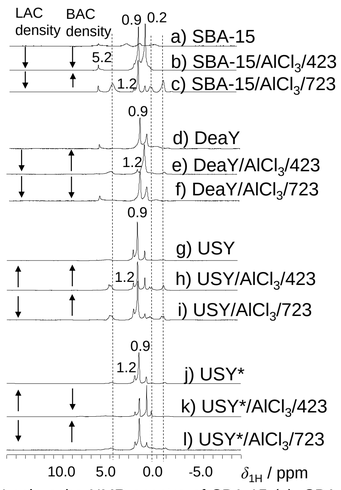

Fig 8: ^{1}H spin echo NMR spectra of SBA-15 (a), SBA-15/$AlCl_3$/423 (b), SBA-15/$AlCl_3$/723 (c), DeaY (d), DeaY/$AlCl_3$/423 (e), DeaY/$AlCl_3$/723 (f), USY (g), USY/$AlCl_3$/423 (h), USY/$AlCl_3$/723 (i), USY* (j), USY*/$AlCl_3$/423 (k) and USY*/$AlCl_3$/723 (l). The dotted line indicates the relative chemical shift of EP shifted to high field due to the non-homogeneous magnetic field at the position of resonating molecules. (The direction of the arrows indicate an increase of acid site density)

The formation of volatile products due to the reaction of EP on the porous SBA-15 without acid site density is very low (Fig. 8a). However, the formation is increased for the modified materials SBA-15/$AlCl_3$/423 and SBA-15/AlC_3/723 with increased acid site density.

Similar to the modified SBA-15, the parent material DeaY with low acid site density forms volatile products. The acid site density of DeaY/$AlCl_3$ /423 and DeaY/$AlCl_3$/723 was increased by the modification. For Al-rich materials, the densities of BAC were decreased by the modification. However, the content of aliphatic volatile products larger than methane increase with high LAC density.

^{1}H MAS NMR spectroscopy

For the investigation of the organic residue on the porous materials ^{1}H MAS NMR spectroscopy was utilized. In Figure 9 a, d, g and j the spectra of EP before and after conversion at 723 K for 10 min on materials under study are shown.

For parent SBA-15 (Fig.9a) and DeaY(Fig. 9d) without acid site density, the cracking of EP is very low. However, with increasing LAC and BAC density of SBA-15/$AlCl_3$/423 and DeaY/$AlCl_3$/423 also the conversion is increased (Figure 9 b and e, respectively). Despite the decreasing BAC density on SBA-15/$AlCl_3$/723 (Fig. 9c) the conversion of EP is due to the high LAC density further increased. For parent and modified USY and USY*, the cracking of EP is high (Fig. 9 g – l). The high acid site densities of this materials causes broad signals of EP and conversion products in the ^{1}H MAS NMR spectra due to the strong interaction of acid sites and organic compounds.

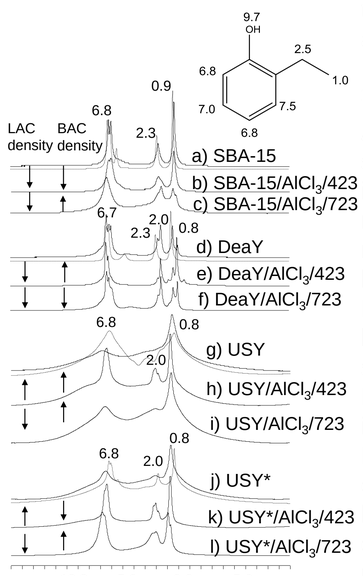

Fig 9: ^{1}H MAS NMR spectra of SBA-15 (a), SBA-15/$AlCl_3$/423 (b), SBA-15/$AlCl_3$/723 (c), DeaY (d), DeaY/$AlCl_3$/423 (e), DeaY/$AlCl_3$/723 (f), USY (g), USY/$AlCl_3$/423 (h), USY/$AlCl_3$/723 (i), USY* (j), USY*/$AlCl_3$/423 (k) and USY*/$AlCl_3$/723 (l). Dotted line indicate 2-ethylphenol on parent materials under study before the reaction. (The direction of the arrows indicate an increase of acid site density)

^{13}C MAS NMR spectroscopy

Additionally, ^{13}C MAS NMR spectroscopy was carried out to investigate the organic residue in materials under study (Fig. 10). For materials with low acid site density, like parent SBA-15 (Fig.10a) and DeaY (Fig. 10d) the conversion is low, evidenced by remaining signals of EP after the reaction. However, the cracking of EP is increased with increasing LAC and BAC density of the materials. The conversion on SBA-15/$AlCl_3$/723 is higher than on SBA-15/$AlCl_3$/423, due to the high LAC density. For parent and modified USY and USY* the complete cracking occur due to the high acid site density. All ^{13}C MAS NMR spectra of the Al-rich materials are very similar. Therefore, the necessary density of acid sites for a complete conversion of EP is lower than the acid site density of parent and modified USY and USY*. The results hints at the influence of LAC density for the cracking of the bio-oil model compound EP due to the increased conversion on materials with LAC as dominating acid sites.

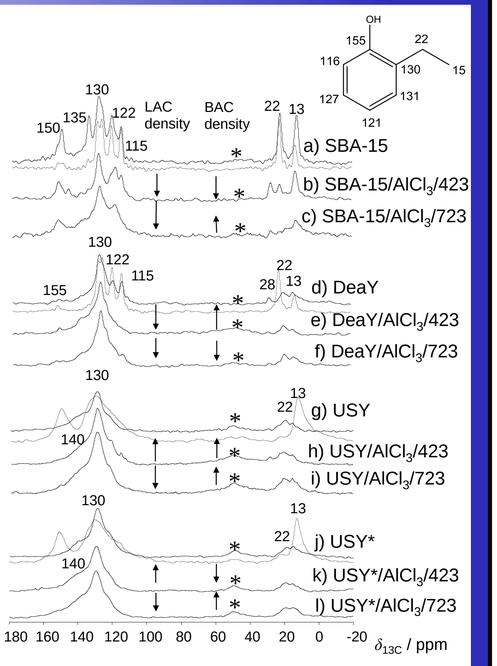

Fig 8: ^{13}C MAS NMR spectra of SBA-15 (a), SBA-15/$AlCl_3$/423 (b), SBA-15/$AlCl_3$/723 (c), DeaY (d), DeaY/$AlCl_3$/423 (e), DeaY/$AlCl_3$/723 (f), USY (g), USY/$AlCl_3$/423 (h), USY/$AlCl_3$/723 (i), USY* (j), USY*/$AlCl_3$/423 (k) and USY*/$AlCl_3$/723 (l). Dotted line indicate 2-ethylphenol on parent materials under study before the reaction. *Asterisks* denote spinning sidebands. (The direction of the arrows indicate an increase of acid site density)

Summary

- Surface acid sites are formed due to $AlCl_3$-modification and thermal treatment of Si-rich materials. Mainly Lewis acid sites (LAC) are formed.
- Al-rich materials like USY and USY* loses Brønsted acid site (BAC) density due to $AlCl_3$-modification and thermal treatment at 723 K in vacuum. However, the Lewis acid site densities are increased.
- Catalytic conversion of 2-ethylphenol (EP) is increased with increased acid site density on Si-rich materials. For Al-rich materials the conversion was complete for all materials.
- Former inactive material SBA-15 showed after the $AlCl_3$-modification and thermal treatment an comparable performance in the catalytic cracking to parent DeaY.
- Due to the $AlCl_3$-modification, the activity in catalytic cracking of EP on DeaY/$AlCl_3$/423 and DeaY/$AlCl_3$/723 was also increased compare to parent DeaY
- The formation of methane as volatile reaction product is low for materials with high LAC density, especially for parent and modified USY and USY*.
- Materials with Lewis acid sites as dominate acid site like SBA-15/$AlCl_3$/723 and DeaY/$AlCl_3$/423 are similar or more active in the catalytic cracking of EP than the same materials with increased BAC density.

References

[1] http://ec.europa.eu/clima/policies/strategies/2020/index_en.htm
[2] Lang S, Benz M, Obenaus U, Himmelmann R, Scheibe M, Klemm E, Weitkamp J, Hunger M, *Top Catal* **2017**. DOI 10.1007/s11244-017-0837-6
[3] Zhao D, Feng J, Huo Q, Melosh N, Fredrickson G, Chmelka B, Stucky G, *Science* **1998** 279:548–552
[4] Černý Z, Macháček J, Fusek J, Casensky B, Kriz O, Tuck DG, *Inorg Chim Acta* **2000** 300–302:556–564

Swen Lang
swen.lang@itc.uni-stuttgart.de
Tel.: +49 711 685 60059
University of Stuttgart
Institute of Chemical Technology

Acknowledgement

We acknowledge the European Union Seventh Framework FP7-NMP-2013, under GA 604277 (FASTCARD) for financing this study